

Nonaxisymmetric Nozzles Installed in Advanced Fighter Aircraft

P. E. Hiley* and H. W. Wallace†
McDonnell Aircraft Company, St. Louis, Mo.

and

D. E. Booz‡
Pratt & Whitney Aircraft, West Palm Beach, Fla.

A study program was conducted to investigate the characteristics of vectoring/reversing nonaxisymmetric nozzles installed in advanced fighter aircraft. Several promising nonaxisymmetric nozzle concepts, ranging from two-dimensional convergent-divergent to two-dimensional plug designs, were evaluated. In addition, a vectoring axisymmetric nozzle was analyzed for comparison. These nozzles were evaluated in aircraft configured for aft-mounted nozzle installations, consisting of a closely spaced, buried nacelle design, and a wide-spaced, podded nacelle design. All incorporated pitch-plane thrust vectoring of $\pm 15^\circ$ and forward-mounted horizontal canards. Some also included thrust-reversing capability. Aircraft performance was evaluated in terms of takeoff gross weight (TOGW) for comparisons of nonaxisymmetric and conventional axisymmetric nozzle installations. The most significant TOGW benefits were achieved when the aircraft sizing point occurred at high lift conditions. Thrust vectoring then could be utilized to reduce wing drag due to lift, decreasing TOGW by up to 6.8%. However, for a mission with an aircraft sizing point occurring at a low lift condition, TOGW penalties of 0.5 to 6.8% were incurred. Combat effectiveness benefits, in terms of aircraft deceleration capability and infrared radiation suppression, also were identified, as were nozzle cost and complexity advantages.

Nomenclature

C_D	= aerodynamic drag coefficient, $D/(q/S_w)$
$C_{D_{\text{axi}}}$	= C_D of baseline aircraft with nonvectoring axisymmetric nozzles
C_{D_i}	= drag due to lift, $D/(qS_w)$
ΔC_{D_N}	= incremental change in $C_{D_{\text{total}}}$ due to jet lift plus supercirculation, at constant α , $\Delta D/(qS_w)$
$C_{D_{\text{total}}}$	= total aircraft C_D ; includes aerodynamic drag plus loss of gross thrust in flight path direction, $\Delta D/(qS_w)$
ΔC_{D_V}	= incremental change in $C_{D_{\text{total}}}$ due to thrust vectoring, at constant $C_{L_{\text{total}}}$, $\Delta D/(qS_w)$
C_{f_g}	= nozzle gross thrust coefficient, F_g/F_{ideal}
C_L	= aerodynamic lift coefficient, $L/(qS_w)$
ΔC_{L_N}	= incremental change in $C_{L_{\text{total}}}$ due to jet lift plus supercirculation, at constant α , $\Delta L/(qS_w)$
$C_{L_{\text{total}}}$	= total aircraft C_L ; includes aerodynamic lift plus gross thrust component normal to flight path direction, $L/(qS_w)$
C_T	= aerodynamic thrust coefficient, $F_g/(qS_w)$, where F_g includes thrust of both engines, if applicable
\bar{c}	= wing mean aerodynamic chord
D	= drag force
F_g	= nozzle gross thrust
F_{ideal}	= nozzle ideal thrust for complete isentropic expansion of actual jet flow to ambient static pressure
IR	= infrared radiation
M_0	= freestream Mach number
NPR	= nozzle pressure ratio; ratio of jet total pressure to ambient static pressure

q	= freestream dynamic pressure
S_c	= canard exposed planform area
S_w	= wing reference area
TOGW	= takeoff gross weight
W	= aircraft or nozzle weight
α	= aircraft angle of attack
Δ	= increment
δ_V	= thrust vector deflection angle
λ	= wavelength

Introduction

THE nonaxisymmetric nozzle offers a number of attractive features for attaining low drag and improved combat effectiveness in high-performance fighter aircraft. Such nozzles integrate well with tapering, nearly rectangular aftbody fuselage contours, thereby offering potential for reducing nozzle/airframe interference drag during cruise. Thrust vectoring can be added to many designs with little added structural weight and complexity. The potential aircraft payoffs for a typical nonaxisymmetric nozzle/integration concept are listed in Fig. 1.

The integration advantages for an aft-mounted two-dimensional plug nozzle installation had been demonstrated previously in wind-tunnel investigations conducted by McDonnell Aircraft Company (MCAIR) and Pratt & Whitney Aircraft (P&WA) during early concept formulation studies on the F-15 aircraft. More recently, deflection of the entire

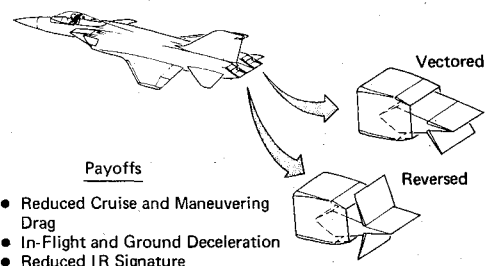


Fig. 1 Nonaxisymmetric nozzle/airframe integration concept and potential aircraft payoffs.

Presented as Paper 75-1316 at the AIAA/SAE 11th Propulsion Conference, Anaheim, Calif., Sept. 29-Oct. 1, 1975; submitted Oct. 7, 1975; revision received July 6, 1976. This work was sponsored by the Air Force Flight Dynamics Laboratory under Contract F33615-74-C-3009.

Index categories: Aircraft Aerodynamics (including Component Aerodynamics); Aircraft Performance.

*Unit Chief, Technology-Propulsion.

†Senior Engineer, Technology-Propulsion. Member AIAA.

‡Assistant Project Engineer, Applied Research Department.

exhaust flow for increasing the lift of a highly swept wing was demonstrated in a wind tunnel investigation at NASA Langley.¹ The lift component of the deflected gross thrust was effectively doubled at Mach 0.9 by increasing wing lift (from supercirculation) due to the induced flowfield associated with the deflected jet. Beneficial application of this supercirculation concept would require application of advanced stability and control technology. A canard configuration probably would be required.

Several design problems, however, are inherent in nonaxisymmetric nozzles. For example, more nozzle cooling is required because of increased wetted area, which can reduce maximum afterburning gross thrust. Furthermore, the non-circular shape reduces structural efficiency, thereby increasing weight.

To further assess the potential of nonaxisymmetric nozzles, the Air Force Flight Dynamics Laboratory sponsored an 18-month analytical study program beginning in November 1973. In this program, MCAIR was the prime contractor, with P&WA as a major subcontractor.

The study program involved two major elements: 1) the formulation and evaluation of practical nonaxisymmetric nozzle and nozzle integration concepts, and 2) evaluation and ranking of these concepts in realistic aircraft systems. Eighty-five different concepts were screened qualitatively, considering cooling requirements, internal performance, weight, drag, complexity, and vectoring/reversing capability. Eighteen specific concepts were chosen from these ideas for installation studies in aircraft systems.

Details of the complete program are discussed in the final report.² This paper summarizes the important results of the study, including evaluation of the eight most promising nozzle/airframe installations.

Baseline Aircraft

The nozzle/airframe installations were derived from two advanced, twin-engine designs with conventional, non-vectoring axisymmetric nozzles. These baseline installations represent a close-spaced, buried nacelle design (TF1) and a wide-spaced, podded nacelle design (TF2) incorporating an inner wing (Fig. 2). A canard was incorporated in the baseline TF1 configuration, as shown in Fig. 2, and was added to the TF2 configurations for this study. Both baseline aircraft employ fly-by-wire control system technology to accommodate an unstable subsonic static margin of approximately -5% \bar{c} and were nearly optimized at this stability level for minimum subsonic maneuvering drag.

The overall geometric characteristics for the two baseline aircraft are similar. They were designed to satisfy the requirements of a subsonic cruise/supersonic weapon delivery mission proposed by the Tactical Air Command for the 1980

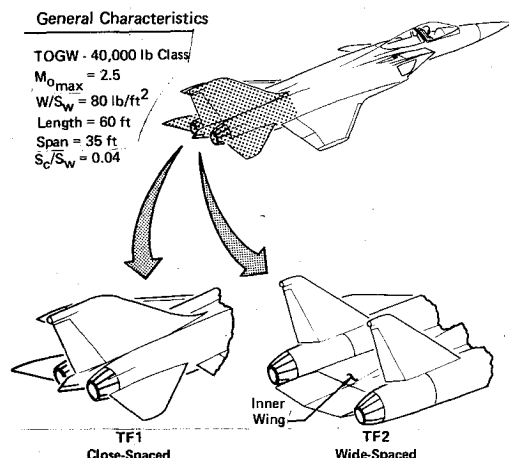


Fig. 2 Baseline axisymmetric nozzle installations.

time period. The study engines were advanced augmented turbofan engines with moderate bypass ratio and a sea-level static airflow of 196 lb/sec.

Study Missions and Aircraft Sizing Points

Two study mission profiles, a Close Air Support Mission and a Maneuverability Mission (Fig. 3), were used in comparative evaluations of the baseline aircraft and the nonaxisymmetric nozzle aircraft designs. The Close Air Support Mission is characterized by low-altitude subsonic cruise, combat, and sustained loiter, and the Maneuverability Mission is characterized by high-altitude subsonic cruise and several 360° , sustained g turn requirements at two transonic flight Mach numbers.

The aircraft configurations were sized to satisfy both mission radius and energy maneuverability (EM) requirements. For the Close Air Support Mission, the Mach 0.9 sustained $-g$ condition was the EM sizing point. The Mach 2.5 ceiling condition was the EM sizing point for the Maneuverability Mission.

Nozzle Design and Performance

Pratt & Whitney Aircraft conducted the nonaxisymmetric nozzle design and performance evaluation, with primary emphasis on minimization of weight and cooling penalties. Nonaxisymmetric nozzles are inherently heavier than axisymmetric designs because of the poor structural efficiency of flat surfaces as pressure vessels. Flat surfaces resist internal pressure loads in bending, which requires a box structure with considerable depth, whereas round structures resist internal pressure loads in tension and require only a thin skin. Furthermore, a two-dimensional shape has more wetted area than a round shape of the same cross-sectional area. This increases the nozzle cooling requirements and hence the losses in afterburning gross thrust.

Nozzle Design and Weights

The baseline axisymmetric $C-D$ nozzle provided a high performance reference for comparative evaluations. This nozzle is an advanced version of the current balanced-beam nozzle for the F100 engine. It is actuated to give the optimum area ratio up to the maximum (2.0), with resultant high in-

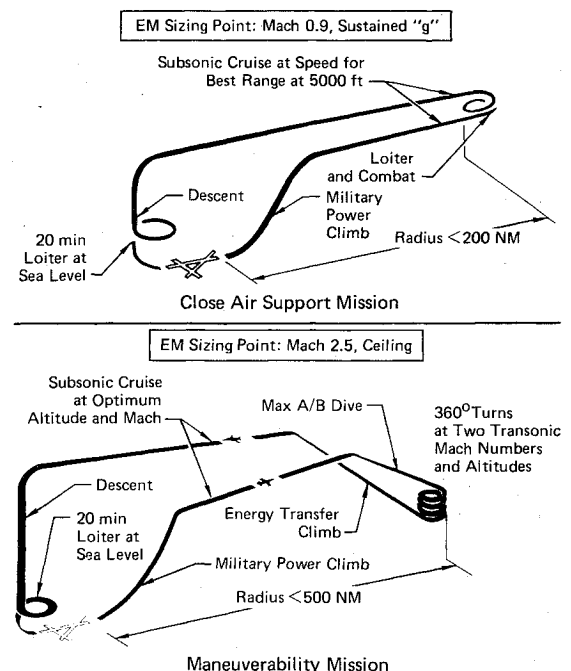


Fig. 3 Study mission profiles.

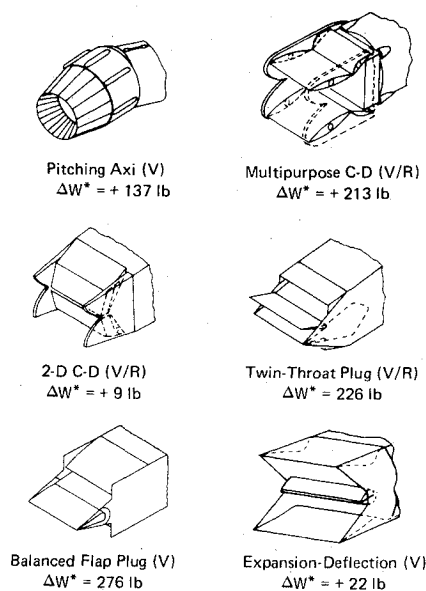


Fig. 4 Nozzle concepts developed.

ternal performance at all flight speeds. The baseline nozzle has a dry power boattail angle of 14° for low boattail drag during subsonic cruise.

The eight most promising nozzle/airframe installations included six different vectoring nozzle concepts. (Two were common to the TF1 and TF2 installation types.) Sketches of these six nozzle concepts are presented in Fig. 4 and include three convergent-divergent and three plug-type nozzles. All except the pitching axisymmetric have a relatively low aspect ratio (nozzle width/nozzle height at throat station) of approximately 4 to 1 at dry power. Nozzle weight estimates relative to the baseline axisymmetric nozzle also are noted. These weights reflect an allowance for strengthening of engine case structure to withstand vectoring/reversing loads, and a 5% development margin.

The pitching axisymmetric *C-D* nozzle is a promising vectoring concept, created by mounting the baseline nozzle on a gimbal ring with two actuators for pitch control. The multipurpose and two-dimensional *C-D* nozzles are nonaxisymmetric concepts incorporating both vectoring and reversing capability. The multipurpose *C-D* nozzle uses four independently actuated flaps for throat area/area ratio control, as well as vectoring and reversing. The two-dimensional *C-D* nozzle, which is shown in the reversed thrust mode in Fig. 4, has much shorter divergent flaps to minimize internal area ratio, making this nozzle best suited for subsonic operation.

The three plug designs illustrated at the bottom of Fig. 4 are attractive concepts due to the lower boattail angles and favorable infrared radiation (IR) suppression characteristics. The twin-throat and balanced-flap designs are similar in that both have exposed two-dimensional plugs. However, the twin-throat design has plug flaps that deflect the exhaust flow for both vectoring and reversing, whereas the balanced-flap design incorporates a completely movable plug tailpiece for vectoring only. The expansion-deflection (*E-D*) design is a unique, light-weight concept with an expanding two-dimensional centerbody located inside of a fixed, outer shroud. Efficient vectoring is achieved by means of a gimbal ring, similar to the pitching axisymmetric design.

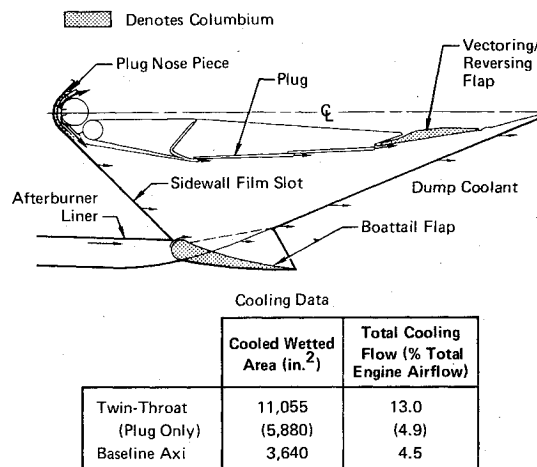


Fig. 5 Cooling system design, twin-throat plug nozzle.

Nozzle Cooling

Design of the cooling system for the flat nozzle sidewalls and the centerbody for the plug concepts received much emphasis in the study. Fan discharge air was utilized as the cooling air source for all applications, thus minimizing degradation of the engine cycle. Columbium was used for the most critical parts of both the baseline and vectoring nozzles, allowing a 450°F increase in operating temperature over conventional nickel-based alloys.

An efficient film/dump cooling scheme was selected for the sidewalls on all nonaxisymmetric concepts except the two-dimensional *C-D* and *E-D*, where film cooling alone was adequate. This cooling concept minimizes cooling flow requirements because the air passages are sized for high coolant velocities. A film discharged from the augmentor liner at the beginning of the sidewalls reduces the heat load to the sidewalls and minimizes the amount of convective coolant required. The convective coolant is dumped axially at the trailing edge of the sidewalls to contribute thrust. The sidewalls also were cut back on the non-plug nozzles to reduce the cooled surface area and reduce weight.

The plug centerbody is a critical cooling area, with special attention required for the plug nose and vectoring/reversing flaps. The complete cooling scheme for the twin-throat plug nozzle is shown schematically in Fig. 5. The plug nosepiece, which is exposed to high-temperature stagnated flow, is formed from columbium and is cooled by convection and by impingement of coolant from the back side. The columbium vectoring/reversing flaps are film-cooled with the plug coolant, whereas the columbium boattail flaps are film-cooled with afterburner liner discharge air.

Nozzle Performance Analysis

In general, the performance of the nonaxisymmetric nozzle concepts was estimated to be 1 to 2% lower at subsonic operating conditions than the high-performance axisymmetric baseline nozzle. The performance comparison is summarized in Fig. 6 at dry power and in Fig. 7 at maximum afterburning (*A/B*) power. These performance estimates were based on available data, where possible, and method of characteristics solutions. Corner flow and sidewall effects were included in the estimate of nozzle thrust coefficient, C_{f_g} . In addition, the effects of cooling flow on maximum afterburning gross thrust were included.

The poorer nozzle efficiency at these subsonic operating conditions generally is due to higher flap divergence angles. The maximum afterburning gross thrust losses due to nozzle cooling (Fig. 7) are due to two causes. First and most important, the cooling air bypasses the augmentor and thus is not available for burning. This reduces the maximum augmented thrust. Second, that portion of the cooling air

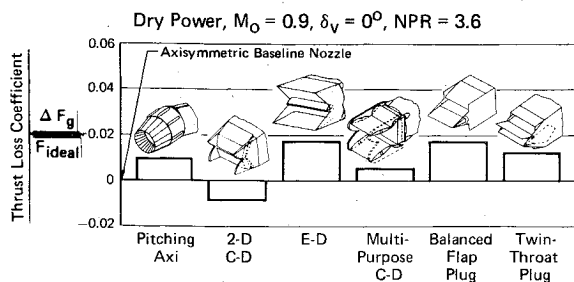


Fig. 6 Estimated nozzle internal performance, subsonic cruise conditions.

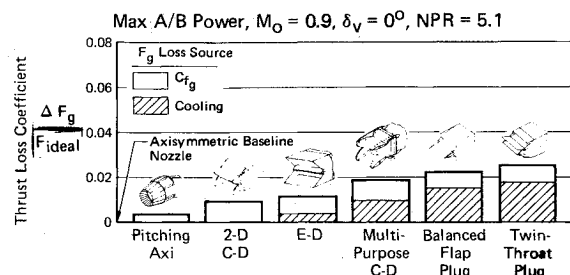


Fig. 7 Estimated nozzle internal performance, subsonic maneuvering conditions.

discharged downstream of the nozzle throat is not accelerated to the full exit velocity of the main exhaust stream. At subsonic maximum afterburning conditions, therefore, cooling losses up to 1.8% of gross thrust are incurred.

Aircraft Performance and System Evaluations

The potential of nonaxisymmetric vectoring nozzles was evaluated by assessing the performance of the entire aircraft system. The eight most promising nozzle/airframe installations considered included five TF1 installations and three TF2 installations. The TF1 nozzle/airframe configurations incorporated the twin-throat plug, balanced-flap plug, pitching axisymmetric, multipurpose $C-D$, and two-dimensional $C-D$ nozzles. The TF2 installations utilized the twin-throat plug, pitching axisymmetric, and expansion-deflection nozzles. Sizing payoffs and penalties were quantified by comparing the TOGW for specified mission and EM requirements. The changes in nozzle performance and weight and in nozzle/airframe drag were determined relative to the baseline axisymmetric configurations. In addition, combat effectiveness payoffs in the areas of IR suppression and deceleration (thrust reversal) also were studied, as well as nozzle production cost.

Nozzle/Airframe Drag Analysis

Improved aircraft performance obtained with nonaxisymmetric nozzle installations results primarily from the cruise drag reduction at dry power associated with superior nozzle/airframe integration, and maneuver drag reduction at A/B power due to thrust vectoring for propulsive-lift advantages. Thrust vectoring can be used most effectively to reduce TOGW, if the aircraft is sized by the subsonic, high-lift EM requirement.

The nozzle/airframe interference drag is reduced because nozzle boattailing is eliminated in the immediate vicinity of nozzle interfairings, tail support boom structure, and empennage surfaces. Nozzle/aft-end flow separation thus is minimized. To evaluate integration drag, both boattail drag and interference drag elements were determined. The boattail drags were based on P&WA data on isolated nozzles, whereas the interference drag estimates were based on available government/industry wind tunnel data on twin-engine nozzle/aft-end installations.

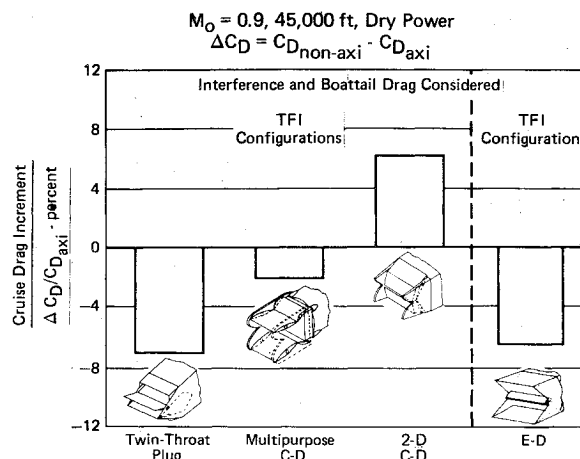


Fig. 8 Estimated cruise drag characteristics.

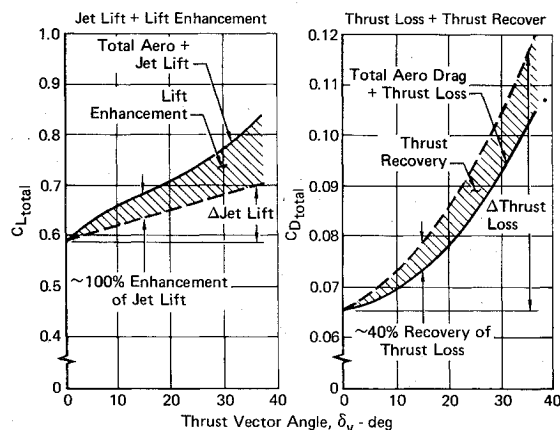
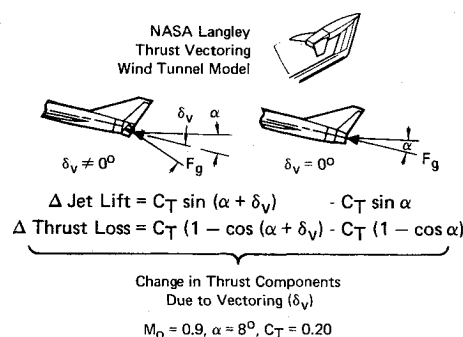


Fig. 9 Effects of thrust vectoring plus supercirculation on lift and drag.

The drag summary shown in Fig. 8 illustrates the important results of the integration drag evaluation. Cruise drag reductions relative to the axisymmetric baseline nozzle installation of up to 7% are indicated for the plug configurations. For the two-dimensional $C-D$ design without a plug centerbody, penalties of 6% of cruise drag were predicted. This is typical for a two-dimensional nozzle design without a centerbody, since the boattail angles are typically higher than an axisymmetric design with the same closure requirements, and higher boattail drag results. Of course, the boattail angle can be reduced by utilizing longer flaps, as in the multipurpose $C-D$ nozzle design. The cruise drag of the multipurpose design is reduced below the two-dimensional $C-D$, as indicated in Fig. 8, but at the expense of about 200 lb in structural weight (Fig. 4).

The most significant drag reductions were obtained by utilizing thrust-induced supercirculation effects for enhancing the wing lift at maneuver conditions. A data base for analyzing these effects was provided by a NASA Langley

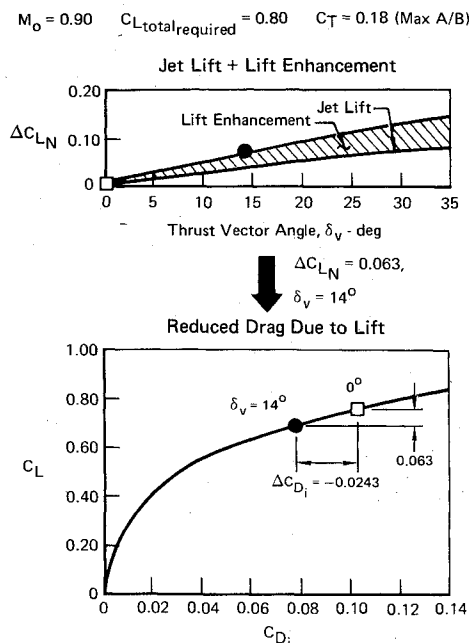
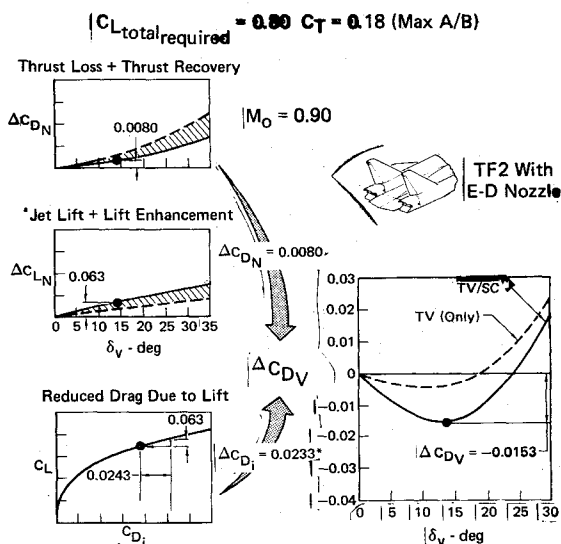


Fig. 10 Utilization of thrust vectoring for augmenting wing/canard lift.

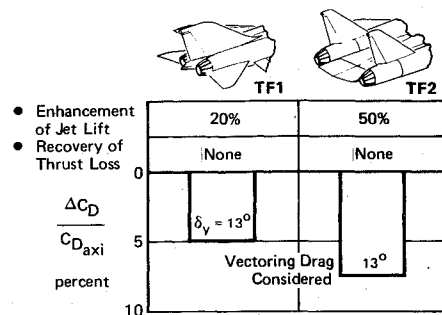


*Includes $\Delta C_D = 0.0010$ trim drag penalty

Fig. 11 Aircraft drag reduction due to thrust vectoring plus supercirculation (TV/SC).

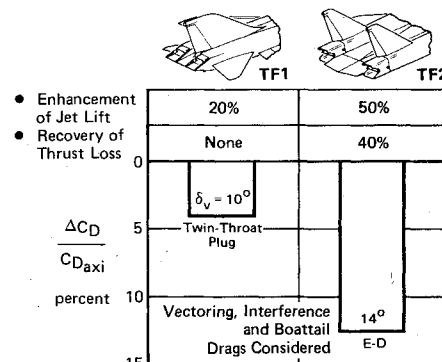
wind tunnel test program,^{3,4} where a partial-span two-dimensional nozzle was used to vector the entire exhaust flow near the trailing edge of a representative fighter wing planform. Typical data at high angle of attack are shown in Fig. 9, indicating enhancement of the component of gross thrust in the lift direction (jet lift) by approximately 100% due to supercirculation effects. A drag decrease due to supercirculation also was observed, wherein the loss component of the deflected gross thrust (in the flight path direction) was reduced by as much as 40% at low vectoring angles. This was due to favorable jet interaction with the wing/body flowfield, generally termed thrust recovery.

The supercirculation effects can be exploited in different ways to improve aircraft performance. In this study, the enhanced jet lift was used to augment the wing/canard lift to meet the sustained normal load factor requirement at the Mach 0.9 EM sizing conditions. This is illustrated in Fig. 10, where the enhanced jet lift and wing/canard lift are combined to give the required total lift coefficient of 0.8 at any thrust



a) Pitching Axisymmetric Nozzle Installations

$$\Delta C_D = C_{D_{pitching\ axi}} - C_{D_{axi}}$$



b) Vectoring Non-Axisymmetric Nozzle Installations

$$\Delta C_D = C_{D_{non-axi}} - C_{D_{axi}}$$

Fig. 12 Estimating maneuvering drag characteristics $M_0 = 0.9$, $C_{L_{total,req}} = 0.8$, $C_T = 0.18$ (max A/B).

vector angle. The wing angle of attack is reduced accordingly to give a significant savings in wing/canard drag due to lift. For the example case of $\delta_v = 14^\circ$, a reduction in drag of $\Delta C_{D_i} = -0.0243$ is thus obtained.

The assessment of the total drag reduction due to vectoring involves evaluating the wing/canard drag reduction in conjunction with drag penalties due to aircraft trimming and thrust loss. Large drag penalties can be incurred if the thrust-vector-induced moments cannot be trimmed with proper (minimum drag) canard deflection. To avoid these drag penalties, the subsonic static margin of the baseline aircraft was relaxed from 5% \bar{c} unstable to a maximum of 15% \bar{c} unstable. Consequently, vectoring benefits could be utilized effectively up to $\delta_v = 10^\circ$ to 15° , with trim drag penalties on the order of only $\Delta C_D \approx 0.0010$.

The analysis used to find the net aircraft drag reduction associated with vectoring is illustrated in Fig. 11 at the EM sizing condition. The case of thrust vectoring without supercirculation is shown for comparison. With thrust vectoring plus supercirculation (TV/SC), the thrust loss at $\delta_v = 14^\circ$ is reduced almost 40%, from $\Delta C_{D_N} = 0.0130$ to 0.0080, because of thrust recovery effects. The jet lift plus lift enhancement provides a ΔC_{L_N} value of 0.063 at this thrust vector angle, thus reducing the required wing/canard lift to a value of $C_L = 0.737$. The drag reduction due to 14° of vectoring is the resultant of the thrust loss plus thrust recovery ($\Delta C_{D_N} = 0.0080$) and the reduced wing/canard drag, including the trim penalty ($\Delta C_{D_i} = -0.0243 + 0.0010$). This results in a net drag reduction of $\Delta C_{D_V} = -0.0233 + 0.0080 = -0.0153$.

The net drag reduction obtained is substantial, even when considering the thrust loss. Furthermore, the maximum drag reduction occurs at a relatively low thrust vector angle; losses in thrust and increases in trim drag become prohibitive at vector angles above about 15° .

A summary of the maneuvering drag changes relative to the baseline aircraft is presented in Fig. 12, indicating drag reduc-

tions up to 13% for the TF2 concepts and about 4% for the TF1 concepts. The lift enhancement and thrust recovery estimates based on the NASA Langley data also are noted, along with the optimum thrust vector angle. The amount of lift enhancement on the TF2 configurations was estimated to be higher than on the TF1 configurations, because of the close proximity of the nozzles to the inner wing lifting surface. These configurations are similar to the NASA test configuration in that both incorporate partial span jets exiting near the trailing edge of a lifting surface. However, since configuration differences exist, the enhancement and recovery factors were estimated conservatively. No thrust recovery benefits were included for the pitching axisymmetric nozzle installations. This was based on the NASA Langley data,³ where it was observed that "even though the augmentation (lift) characteristics of the round nozzles were comparable with the rectangular exits, the round exits exhibited much poorer thrust recovery characteristics."

Aircraft Performance Estimates

Aircraft TOGW was estimated for each configuration to determine the combined effects of changes in nozzle performance, nozzle/airframe structural weight, and nozzle/airframe drag. The individual contributions to TOGW of these three parameters were calculated at each of the important mission legs and at the EM sizing points.

A summary of the total TOGW increments for the eight nonaxisymmetric configurations is presented in Fig. 13 for the Close Air Support and Maneuverability Missions. Aircraft size reductions are greater on the Close Air Support Mission for the TF2 nozzle installations, primarily because of the drag reduction at the subsonic EM sizing point. The benefit is highest on the TF2 with the *E-D* nozzle, about 2700 lb (6.8%) TOGW reduction, because both nozzle internal performance and structural weight penalties were the lowest. The drag reductions associated with thrust vectoring on the TF2 concepts are not effective in reducing TOGW on the Maneuverability Mission. This occurs because the aircraft are sized by the Mach 2.5 ceiling requirement at a normal load factor condition requiring low lift coefficient. The TF1 concepts incur from 200 to 2700 lb (0.5 to 6.8%) TOGW penalties on the two missions because of higher structural weights, lower nozzle performance, and less favorable supercirculation advantages.

As discussed previously, the maximum cruise drag reduction obtained with nonaxisymmetric nozzles was significant, about 7% of total aircraft drag. However, the lower cruise

drag did not contribute significantly to TOGW reductions (about 500 lb maximum). This occurred because the sensitivity of TOGW to cruise drag was relatively low for the study missions.

Deceleration, IR Suppression, and Cost Benefits

The results of the comparative analyses indicate that well-designed nonaxisymmetric nozzles with vectoring capability offer potential to reduce aircraft size for constant mission and EM requirements. Payoffs were also identified in the areas of aircraft deceleration, IR suppression, and nozzle production cost.

Thrust reversal/modulation provides rapid deceleration capability, without requiring aerodynamic speedbrakes, for in-flight operations. This improved operational capability was evaluated for the TF1 aircraft with the vectoring/reversing twin-throat plug nozzle installation, as shown in Fig. 14. The in-flight deceleration increment provided by the thrust reverser was at least 200% greater up to Mach 0.9 than that provided by the 10-ft² speedbrake of the baseline TF1. This relatively small speedbrake was the maximum size for practical integration with the airframe on this aircraft. However, the deceleration increment for a 30-ft² speedbrake, which is more typical of current fighter aircraft, also was computed. The thrust reverser was still superior, as shown in Fig. 14. Furthermore, unlike the speedbrake, the thrust reverser remains effective at low speeds.

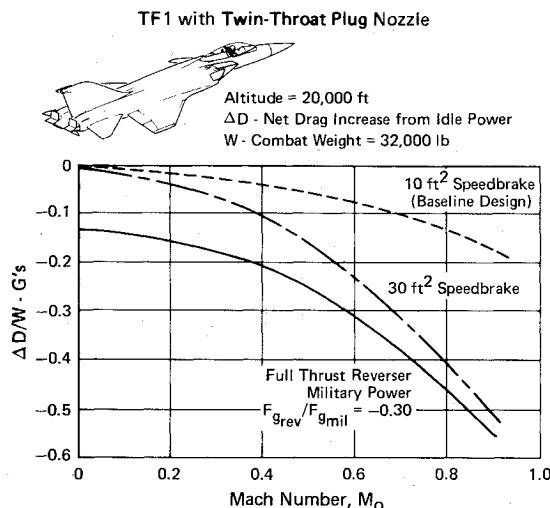


Fig. 14 Deceleration capability with thrust reversing.

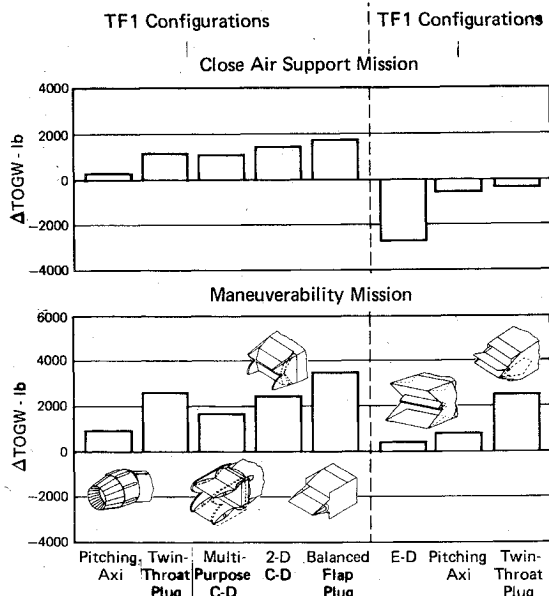


Fig. 13 Mission performance/sizing results.

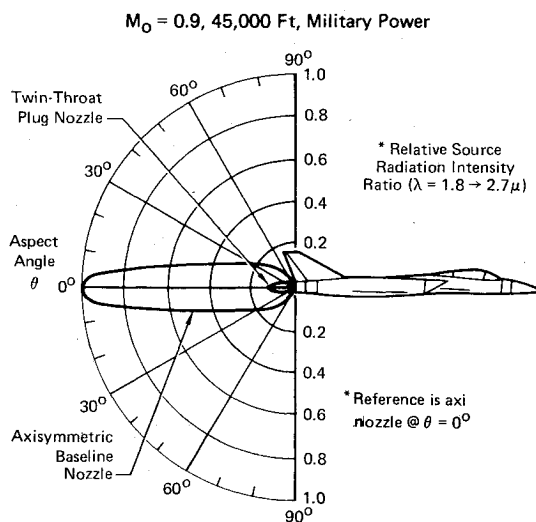


Fig. 15 Reduced IR lock-on range with twin-throat plug nozzle.

It should be noted that the thrust reverser efficiency used in the Fig. 14 illustration, $F_{grev}/F_{gml} = -0.3$, is based on static test data. As flight speed increases, significant additional deceleration force can be obtained by interaction of the reversed jet with the nozzle/aft-end flowfield and from base drag on the rear of the reverser flaps. Therefore, the net deceleration force at the high subsonic, reversed-thrust conditions is conservative in this example.

Increased aircraft survivability due to lower IR signature is another potential advantage of nonaxisymmetric nozzles. The greatest gains in IR suppression are for two-dimensional nozzles with cooled centerbodies, which block much of the radiation emitted by the hot turbine parts. The IR signatures of the twin-throat plug nozzle and the baseline axisymmetric nozzle are compared in Fig. 15. An estimated 90% IR signature reduction can be achieved at rearward aspect angles, which converts to 45% reduction in IR lock-on range.

The design simplicity of nonaxisymmetric nozzles can result in significant reductions in nozzle production costs. For example, there are only 18 major components in the vectoring/reversing multipurpose $C-D$ nozzle design, compared to 110 for the conventional axisymmetric $C-D$ nozzle on the P&WA F100 engine for the F-15 aircraft. The major payoff is a 33% reduction in the estimated production cost of the nozzle. This assumes the use of columbium in the multipurpose nozzle to reduce the cooling penalty.

Summary

The most significant benefits identified for vectoring nonaxisymmetric nozzles were aircraft sizing benefits, where thrust vectoring plus supercirculation could be utilized at the high-lift EM condition to obtain a TOGW reduction of up to 6.8%. However, at the low-lift coefficients associated with the supersonic EM condition, thrust vectoring benefits were

negligible, and TOGW penalties were incurred due to nozzle performance and structural weight penalties.

The study results further showed that the following potential improvements, relative to conventional axisymmetric nozzles, are possible: 1) up to 7% lower cruise drag due to improved nozzle/airframe integration; 2) increased aircraft survivability due to IR signature reductions of up to 90% with plug nozzles; 3) vectoring/reversing capability with less complexity; and 4) reductions in nozzle production cost of 33%.

Considerable further effort is necessary to verify these potential payoffs for a future fighter aircraft. Studies should be conducted involving subscale nozzle internal performance, IR, and cooling experiments, as well as wind tunnel tests on practical nozzle/airframe installations. These results then should be utilized to determine system payoffs on aircraft configurations specifically designed for thrust vectoring/reversing nonaxisymmetric nozzles. Furthermore, prior to low-risk usage of such nozzle systems in future aircraft, full-scale ground and flight-test demonstrations also would be required.

References

- ¹Corson, B. W., Jr., Capone, F. J., and Putnum, L. E., "Lift Induced on a Swept Wing by a Two-Dimensional Partial Span Jet at Mach Numbers from 0.2 to 1.3," NASA TM X-2309, 1971.
- ²Hiley, P. E. and Wallace, H. W., "Investigation of Non-Axisymmetric Nozzles Installed in Tactical Aircraft," Air Force Flight Dynamics Laboratory, Wright-Patterson Air Force Base, Ohio, AFFDL-TR-75-61, June 1975.
- ³Capone, F. J., "Supercirculation Effects Induced by Vectoring a Partial-Span Rectangular Jet," *Journal of Aircraft*, Vol. 12, Aug. 1975, pp. 633-638.
- ⁴Capone, F. J., "Lift Induced Due to Thrust Vectoring of a Partial-Span Two-Dimensional Jet at Mach Numbers from 0.4 to 1.3," Addendum to NASA Langley Research Center Working Paper LWP-1116, NASA, Aug. 28, 1974.

From the AIAA Progress in Astronautics and Aeronautics Series . . .

AEROACOUSTICS: JET AND COMBUSTION NOISE; DUCT ACOUSTICS—v. 37

Edited by Henry T. Nagamatsu, General Electric Research and Development Center; Jack V. O'Keefe, The Boeing Company; and Ira R. Schwartz, NASA Ames Research Center

A companion to Aeroacoustics: Fan, STOL, and Boundary Layer Noise; Sonic Boom; Aeroacoustic Instrumentation, volume 38 in the series.

This volume includes twenty-eight papers covering jet noise, combustion and core engine noise, and duct acoustics, with summaries of panel discussions. The papers on jet noise include theory and applications, jet noise formulation, sound distribution, acoustic radiation refraction, temperature effects, jets and suppressor characteristics, jets as acoustic shields, and acoustics of swirling jets.

Papers on combustion and core-generated noise cover both theory and practice, examining ducted combustion, open flames, and some early results of core noise studies.

Studies of duct acoustics discuss cross section variations and sheared flow, radiation in and from lined shear flow, helical flow interactions, emission from aircraft ducts, plane wave propagation in a variable area duct, nozzle wave propagation, mean flow in a lined duct, nonuniform waveguide propagation, flow noise in turbofans, annular duct phenomena, freestream turbulent acoustics, and vortex shedding in cavities.

541 pp., 6 x 9, illus. \$19.00 Mem. \$30.00 List

TO ORDER WRITE: Publications Dept., AIAA, 1290 Avenue of the Americas, New York, N. Y. 10019